THE JOURNAL OF PHYSICAL CHEMISTRY B

Article

pubs.acs.org/JPCB

AMBER Empirical Potential Describes the Geometry and Energy of Noncovalent Halogen Interactions Better than Advanced Semiempirical Quantum Mechanical Method PM6-DH2X†

Mahmoud A. A. Ibrahim*,‡,§

‡School of Chemistry, University of Manchester, Oxford Road, Manchester M139PL, United Kingdom

§Chemistry Department, Faculty of Science, Minia University, Minia 61519, Egypt

Supporting Information

ABSTRACT: A recently published study on halogen bonding in casein kinase 2 (CK2)-inhibitor complexes claimed that the halogen-bond-corrected PM6 semiempirical method (PM6-DH2X) describes the halogen bonding properties correctly, whereas the AMBER empirical potential fails. The current study employs our positive extra-point (PEP) approach for halogen bonding, in which the σ-hole on the halogen atom is represented by an extra point of charge. The performance of the two methods in describing halogen bonding in halobenzene···Lewis base and CK2-inhibitor complexes was reassessed. Compared to basis set superposition error- (BSSE-) corrected MP2/aug-cc-pVDZ (with PP functions on the Br and I atoms) data, the AMBER force field described the halogen bonding in halobenzene···Lewis base complexes slightly better than the PM6-DH2X method. Fifteen polyhalogenated benzimidazole inhibitors (taken from a study of Dobeš et al.) complexed to CK2 protein were studied. The binding energies were calculated using the molecular mechanical–generalized Born surface area (MM-GBSA) approach. Compared to the corresponding experimental data, the AMBER force field yielded much better results than the PM6-DH2X method. Finally, the performance of both methods in describing C–X···π-system and C–X···H–O/C interactions was examined. A comparison with MP2 data revealed that the PM6-DH2X method failed to describe them, whereas the AMBER force field performed well.

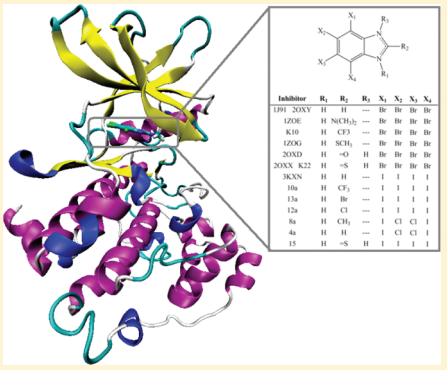

INTRODUCTION

The role and application of participating halogen atoms (X) in directional noncovalent interactions with a Lewis base (B) have recently attracted considerable interest in the fields of drug discovery and crystal engineering.[1−4] The potential of halogen atoms in this electrostatic interaction, called the halogen bond, returns to the presence of an electropositive region (called the σ-hole) on the A–X axis formed by the anisotropic distribution of charge density on the halogen atom.[5−7] The strength of the halogen bond is comparable to that of the hydrogen bond and increases with increasing σ-hole magnitude (I > Br > Cl).[8−10]

Theoretical studies are essential for investigating the characteristics and properties of halogen bonds.[7,11−16] The accuracy of theoretical methods of predicting halogen bond properties such as bond length and energy has been evaluated to a certain degree.

Among quantum mechanical methods, the Hartree–Fock (HF) method has been found to underestimate the halogen bond energy compared to the coupled-cluster with single and double and perturbative triple excitations [CCSD(T)] method because the former neglects electron correlations.[17−19] However, the second-order Møller–Plesset (MP2), third-order Møller–Plesset (PM3), and quadratic configuration interaction with single and double excitation (QCISD) methods overestimate the halogen bond energy compared to the CCSD(T) method, and the halogen bond energy difference depends on the nature of the halogen and Lewis base atoms.[17−19] Among density functional theory functionals, PBEKCIS, B97–1, MPWLYP, and M06–2X functionals have been found to yield results similar to those of very expensive *ab initio* methods such as CCSD(T) and MP2.[20,21] A large basis set including high-levels of correlation and multiple polarization functions is usually essential for accurate estimation of the interaction energies of halogen-bonded complexes.[22]

Among semiempirical methods, semiempirical quantum mechanical methods—MNDO, MNDO-*d*, AM1, RM1, PM3, and PM6—failed to accurately describe the energy and geometry of halogen bonding.[23] The failure of the most advanced semiempirical method, PM6,[24,25] to describe halogen bonding is attributed to underestimation of the core–core repulsion term; a very short halogen bond is thus predicted between the halogen atom and the Lewis base, which in turn leads to overestimation of the halogen bond energy.[26] A correction

Received: January 12, 2012
Revised: February 11, 2012
Published: March 6, 2012

dx.doi.org/10.1021/jp3003905 | J. Phys. Chem. B 2012, 116, 3659–3669

energy term was recently proposed to correct the halogen bonding in the PM6 method.[26]

Dobeš et al. compared the performance of dispersion- and hydrogen- and halogen-bond-corrected PM6 (PM6-DH2X) method in describing halogen bonding in casein kinase 2 (CK2) -inhibitor complexes to that of the corresponding AMBER force field.[27] They claimed that PM6-DH2X described halogen bonding well, whereas the AMBER force field failed.[27]

The current study reassesses the performance of the AMBER force field and PM6-DH2X in describing halogen bonding. In the AMBER empirical calculations, we employed our developed positive extra-point (PEP) approach in which the σ-hole on the halogen atom is represented by an extra-point of positive charge.[28] The performance assessment was based on three types of calculations. First, we described the bond length and strength in small halogen-bond-forming complexes such as halobenzene molecules complexed to formaldehyde, furan, pyridine, and ammonia molecules. The calculated empirical and semiempirical halogen bond lengths and energies were compared to the corresponding high-level quantum mechanical data. Second, we predicted the binding affinity of halogen-containing inhibitors toward CK2 protein. The empirical binding energies were calculated using the molecular mechanical−generalized Born surface area (MM-GBSA) approach on the basis of the molecular mechanical energy−minimized single-structure (MM-GBSA//MM-SS) and ensemble of molecular dynamics generated structures (MM-GBSA//MM-MD). The calculated binding energies were compared to the corresponding PM6-DH2X data from Dobeš et al. and experimental data. Third, we described the noncovalent interactions between halogens and small biologically important molecules such as water and aromatic rings, that are, C−X···H−O/C and C−X···π-system interactions. The potential energy dissociation curves of halobenzene···benzene (C−X···π-system), benzene···halobenzene (C−X···H−C), and halobenzene···water (C−X···H−O) complexes were generated and compared to the corresponding high-level quantum mechanical data.

METHODS

Potential Energy Surface Calculations. In the current study, the length and strength of halogen bonds between halobenzene molecules and four Lewis bases (O_{sp^2}, formaldehyde; O_{sp^3}, furan; N_{sp^2}, pyridine; and N_{sp^3}, ammonia) were investigated. The monomers forming the complexes were first optimized by the MP2 method[29] using a mixed basis set scheme in which bromine and iodine atoms were treated with the augmented correlation-consistent valence double-ζ basis set with a polarization function (aug-cc-pVDZ-PP);[30,31] all other atoms, including chlorine, were treated with the aug-cc-pVDZ[30] basis set. The monomers were then held fixed during the prospective calculations. The potential energy surfaces were generated along the halogen···Lewis base bonds at the MP2/aug-cc-pVDZ level (with PP functions on the Br and I atoms), PM6-DH2X level, and AMBER empirical level. This calculation protocol previously yielded an energy difference value ~0.02 kcal/mol higher than that of the fully optimized complex.[32] Note that the angle of the halogen bond (i.e., C−X···Lewis base) was maintained at 180.0° to decrease any possible noncovalent interactions between the halogen atom and the other Lewis base atoms.

At the MP2 level, the basis set superposition error (BSSE) was taken into account and corrected using the Boys and Bernardi counterpoise method.[33] All the MP2 calculations were performed using Gaussian03 software.[34]

For the AMBER empirical calculations, the electrostatic potential of the studied molecules was generated at the HF/6-31G* level while bromine and iodine atoms were treated using the aug-cc-pVDZ-PP basis set. The atomic partial charges were then evaluated with incorporating an extra-point of charge on each inhibitor's halogen atom using the restrained electrostatic potential (RESP) approach.[35] The parameters used for the extra-point were taken from our previous study.[28] The atomic partial charges for hydrogen and carbon atoms in the benzene molecule were taken from a previous study: $q(\mathrm{HA}) = -q(\mathrm{CA}) = 0.115$.[36] In addition, the atomic partial charges and atom types for the water molecule were taken from the TIP3P molecule.[37] All the empirical calculations were done using the MM standalone program implemented in Gaussian03.[34]

For PM6-DH2X calculations, the single-point energies were calculated using PM6-DH2 with the help of MOPAC2009 software;[38] the halogen-bond-correction term was added as defined by Řezáč et al.[26]

$$E_{PM6-DH2X} = E_{PM6-DH2} + E_{X-correction}$$

$$E_{X-correction} = ae^{-br}$$

where a and b are constants that depend on the halogen and Lewis base atoms, and r is the halogen···Lewis base distance.

CK2-Inhibitor Complexes. *Inhibitor Preparation.* Fifteen polyhalogenated benzimidazole derivatives taken from the work of Dobeš et al. were studied: seven inhibitors from test set A and eight from test set B. All were randomly selected. Their chemical structures are shown in Figure 1. The same

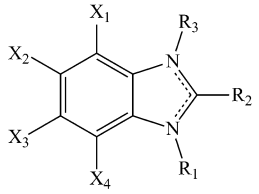

Inhibitor	R_1	R_2	R_3	X_1	X_2	X_3	X_4
1J91 2OXY	H	H	---	Br	Br	Br	Br
1ZOE	H	$N(CH_3)_2$	---	Br	Br	Br	Br
K10	H	CF3	---	Br	Br	Br	Br
1ZOG	H	SCH_3	---	Br	Br	Br	Br
2OXD	H	=O	H	Br	Br	Br	Br
2OXX K22	H	=S	H	Br	Br	Br	Br
3KXN	H	H	---	I	I	I	I
10a	H	CF_3	---	I	I	I	I
13a	H	Br	---	I	I	I	I
12a	H	Cl	---	I	I	I	I
8a	H	CH_3	---	I	Cl	Cl	I
4a	H	H	---	I	Cl	Cl	I
15	H	=S	H	I	I	I	I

Figure 1. Chemical structures of the studied CK2 inhibitors.

nomenclature is used for the studied inhibitors as in the original paper to facilitate comparison.[27]

For atomic charge assignment, the inhibitors were optimized at the B3LYP/6-311+G** level[39−41] with the aug-cc-pVDZ-PP basis set for bromine and iodine atoms. The atomic charges were, then, assigned using the RESP approach.

dx.doi.org/10.1021/jp3003905 | J. Phys. Chem. B 2012, 116, 3659−3669

CK2-Inhibitor Complex Preparation. We used almost the same protocol as that used by Dobeš et al. to prepare the CK2-inihbitor complexes. The molecular structures of the complexes were downloaded from the RCSB protein bank (http://www.pdb.org). If a PDB file is unavailable for the inhibitors in complex with CK2 protein, test set B, the crystal structure of CK2 complexed with ANP (PDB code: 1JWH[42]) was used as a template for constructing the missing molecular systems, and the inhibitors were placed at the active site positioned so as to form a halogen bond with the carboxyl oxygen of the amino residues. If two CK2 units present in the PDB file, only one was taken into account, and the second was deleted. The protonation state of the studied complexes was examined, and any missing hydrogen atoms were added.

For single-structure calculations, all the crystallic water molecules and metal ions were deleted. However, for the MD simulations, they were retained; in addition, chloride ions were added to the complexes as required yielding a neutral charge overall, and the molecular systems were then solvated with TIP3P water molecules.[37]

Single-Structure Calculation. Here, single-structure refers to the crystal structure, if available, or the manually docked structure of the CK2-inhibitor complexes. In molecular mechanical minimization for single-structure (MM-SS) calculations, the truncated Newton linear conjugate gradient method with LBFGS preconditioning[43] was used. The convergence criterion for the energy gradient was 10^{-12} kcal/mol Å. A cutoff value of 999 Å and a generalized Born solvent model were used. No periodic boundary condition was applied. A weak constrain was applied to the inhibitor during minimization. The latter condition is necessary because of the limitation of treating the placed extra-point on the halogen atom as a point of charge (i.e., not a real atom) in implicit-solvent minimization in AMBER code.[44] All the empirical minimizations of the CK2-inhibitor complexes were conducted using the sander program implemented in the AMBER package.[44]

Molecular Dynamics. A molecular mechanical simulation of the CK2-inhibitor complexes was conducted using the AMBER software.[44] AMBER force field 99SB,[45] and the general AMBER force field (GAFF)[46] were used to describe the studied inhibitors and the proteins including the solvent molecules, respectively. The molecular CK2-inihibitor complexes were initially energy−minimized and then gradually heated to 300° K over 50 ps with a weak constrain of 10 kcal/mol.Å^2 applied to the protein. The systems were equilibrated for 500 ps before the production stage. The data were then collected over a 2 ns simulation. The time step was set to 2 fs and all bonds involving hydrogen atoms were constrained using the SHAKE option during the MD simulation.

Binding Energy. The binding energy for a CK2-inhibitor complex of reaction type

$$\text{protein} + \text{inhibitor} \rightarrow \text{protein−inhibitor}$$

is estimated by

$$\Delta G = -RT \ln k_i$$
$$= G_{complex} - (G_{protein} + G_{inhibitor})$$

or

$$= \bar{G}_{complex} - (\bar{G}_{protein} + \bar{G}_{inhibitor})$$

where the overbar represents the ensemble average.

In the current study, the binding energy was calculated using MM-GBSA on the basis of MM-SS, and uncorrelated snapshots collected every 10 ps over the 2 ns production run from the MD simulation (MM-MD). The coordinates of each inhibitor, receptor, and complex were extracted from a single trajectory (called the single-trajectory approach). For MM-GBSA, the energy term G (analogous to the $\bar{G}$ used in ensemble calculations) was estimated as

$$G = E_{\text{int}} + E_{vdw} + E_{elec} + G_{GB} + G_{SA} - TS$$

where E_{int}, E_{vdw}, and E_{elec} are the internal, van der Waals, and electrostatic solute energies, respectively. G_{GB} is the electrostatic solvation free energy, given by $G_{GB} = G_{\varepsilon = 78.3} - G_{\varepsilon = 1}$.

G_{SA} is the nonpolar contribution to the solvation free energy from the solvent-accessible surface area (SASA), given by: $G_{SA} = 0.00542 \times \text{SASA} + 0.92$.[47]

TS is the configurational entropy. For the MM-GBSA binding energies, the entropy of the inhibitors was neglected.

For the PM6-DH2X level, the binding energies were taken from Dobeš et al.[27] and are referred to here as the PM6-DH2X binding energies. Here, we summarized the protocol used by Dobeš et al. to calculate the binding energy for the purpose of comparison. The CK2-inhbitor complexes were fully optimized using the PM6-DH2X level in an implicit solvent medium with the help of the continuum COSMO model implemented in the MOPAC code. The binding energies $\Delta G'_w$ were then calculated; they are given by

$$\Delta G'_w = \Delta H_w + \Delta E_{def}(I) + \Delta E_{def}(P) + \Delta\Delta G_w(I) + \Delta\Delta G_w(P) - T\Delta S_w$$

where ΔH_w is the interaction enthalpy. $\Delta E_{def}(I)$ and $\Delta E_{def}(P)$ are the inhibitor (I) and protein (P) deformation energies, respectively, given by

$$\Delta E_{def}(I) = E(I)_w^{PI} - E(I)_w^{I}$$

$$\Delta E_{def}(P) = E(P)_w^{PI} - E(P)_w^{P}$$

where the superscripts PI, I, and P represent the inhibitor (or protein) conformation in a protein-inhibitor complex, the conformation of the relaxed inhibitor, and the protein conformation in water, respectively.

$\Delta\Delta G_w(I)$ and $\Delta\Delta G_w(P)$ are the inhibitor (I) and protein (P) solvation free energy correction terms, respectively. They are estimated as the difference between the solute solvation energy calculated by the COSMO model using the PM6-DH2X level and the MOPAC code and by the C-PCM model using the B3LYP/6-31G* (or B3LYP/SDD for iodinated inhibitor) level and the Gaussian software.

$$\Delta\Delta G_w(I) = \Delta G_w^{MOPAC}(I)^{PI} - \Delta G_w^{Gaussian}(I)^{PI}$$

$$\Delta\Delta G_w(P) = \Delta G_w^{MOPAC}(P)^{PI} - \Delta G_w^{Gaussian}(P)^{PI}$$

$T\Delta S_w$ is the interaction entropy.

RESULTS AND DISCUSSION

Halogen···Lewis Base Complexes. The bond length and energy of halogen bonds in halobenzene molecules complexed to four different Lewis bases (formaldehyde, furan, pyridine, and ammonia) were estimated at the PM6-DH2X and AMBER empirical levels. The potential energy curves along the

dx.doi.org/10.1021/jp3003905 | J. Phys. Chem. B 2012, 116, 3659−3669

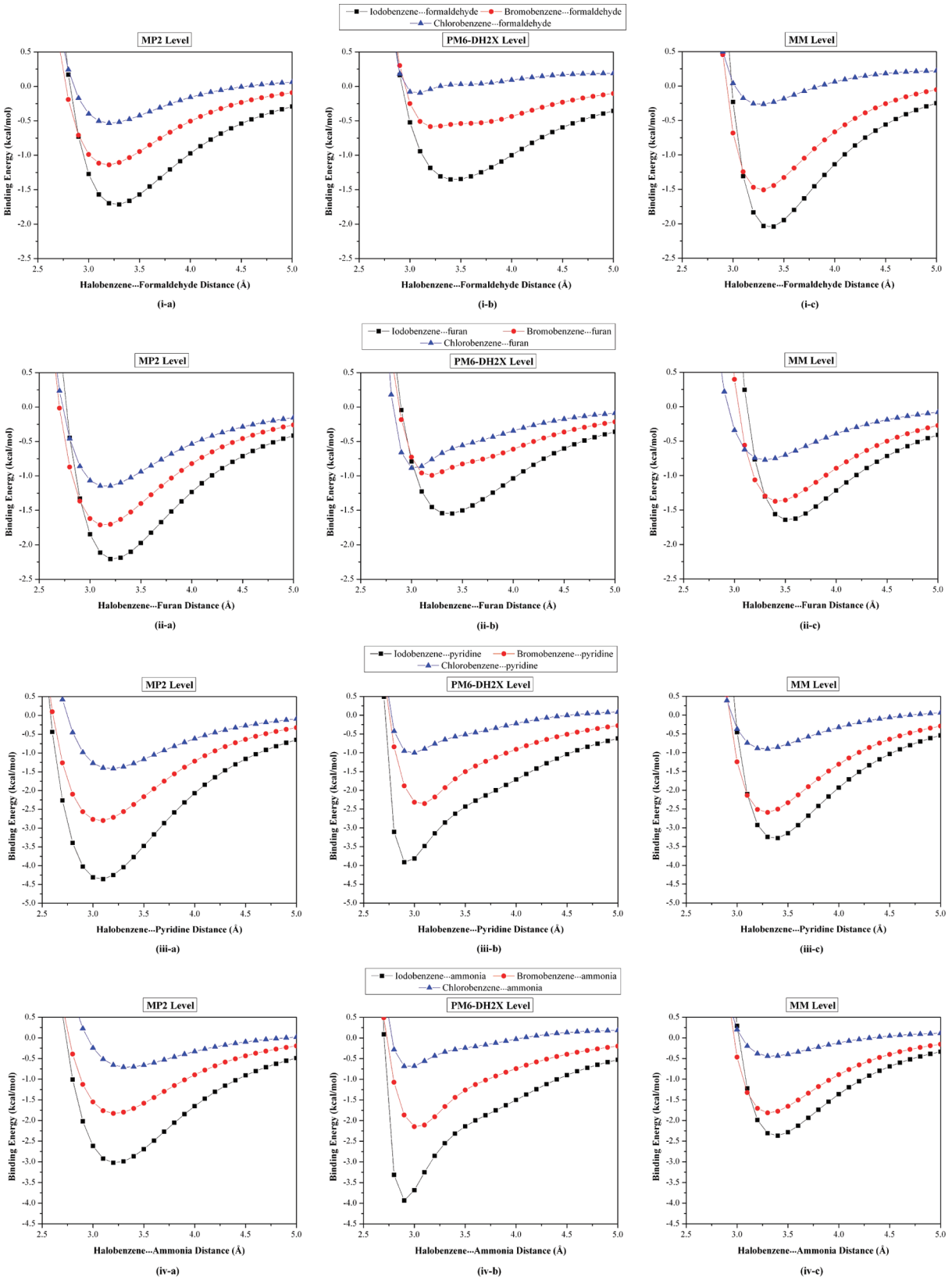

Figure 2. Potential energy curves for halogen bond dissociation in halobenzene complexed to (i) formaldehyde, (ii) furan, (iii) pyridine, and (iv) ammonia, calculated (a) at BBSE-corrected MP2/aug-cc-pVDZ level (with PP functions on the Br and I atoms), (b) by PM6-DH2X method, and (c) by AMBER force field.

halogen···Lewis base bond for the complexes were evaluated with an interval value of 0.10 Å. Figure 2 shows the generated graphs. The halogen bond length and energy of the corresponding local minima were calculated to two decimal

dx.doi.org/10.1021/jp3003905 | J. Phys. Chem. B 2012, 116, 3659−3669

Table 1. Calculated halogen bond lengths of, and binding energies for, the studied halobenzene···Lewis base complexes

	halogen bond length (Å)			halogen bond energy (kcal/mol)		
complex	MP2[a]	PM6-DH2X	AMBER	MP2[a]	PM6-DH2X	AMBER
chlorobenzene···formaldehyde	3.21	3.06	3.26	−0.53	−0.10	−0.27
chlorobenzene···furan	3.15	3.03	3.30	−1.15	−0.89	−0.77
chlorobenzene···pyridine	3.17	2.97	3.26	−1.42	−1.01	−0.90
chlorobenzene···ammonia	3.33	2.94	3.34	−0.71	−0.71	−0.44
rms error[b]		0.24	0.09		0.32	0.37
bromobenzene···formaldehyde	3.18	3.23	3.28	−1.14	−0.59	−1.51
bromobenzene···furan	3.14	3.17	3.43	−1.72	−0.99	−1.38
bromobenzene···pyridine	3.07	3.06	3.29	−2.80	−2.37	−2.59
bromobenzene···ammonia	3.21	3.03	3.31	−1.83	−2.16	−1.82
rms error[b]		0.09	0.20		0.53	0.27
iodobenzene···formaldehyde	3.27	3.43	3.35	−1.72	−1.35	−2.05
iodobenzene···furan	3.23	3.35	3.53	−2.21	−1.55	−1.65
iodobenzene···pyridine	3.07	2.93	3.36	−4.36	−3.93	−3.29
iodobenzene···ammonia	3.22	2.90	3.38	−3.03	−3.93	−2.37
rms error[b]		0.20	0.23		0.63	0.71
total rms error[b]		0.19	0.18		0.51	0.49

[a]A mixed basis set scheme was used: aug-cc-pVDZ-PP for iodine and bromine atoms, and aug-cc-pVDZ for all other atoms. BSSE was considered in the MP2 calculations. [b]The rms error was calculated with respect to the MP2 level.

Table 2. Calculated Binding Energies, and Binding Energy Components, for the Studied CK2-Inibitor Complexes at PM6-DH2X and AMBER Empirical Levels[a]

Test Set A

	CK2-Inhibitor Binding Energy								
Inhibitor	PM6-DH2X[b]					AMBER		K_i (μM)[b]	ΔG_{exp}
	ΔH_w	$\Delta\Delta G_w$(I)	ΔE_{def}(I)	$T\Delta S_w$	$\Delta G'_w$	MM-GBSA//MM-SS[c]	MM-GBSA//MM-MD		
1J91	−15.13	−4.70	0.67	−15.67	−3.49	−41.48	−28.51	0.400	−8.72
1ZOE	−38.09	−7.16	0.87	−19.53	−24.85	−38.27	−31.35	0.045	−10.01
1ZOG	−28.81	−6.80	1.04	−18.83	−15.74	−37.09	−30.52	0.070	−9.75
2OXD	−22.29	−5.25	0.83	−10.62	−16.09	−33.39	−29.11	0.150	−9.30
2OXX	−16.68	−10.43	0.93	−3.09	−23.09	−34.30	−28.75	0.200	−9.13
2OXY	−20.87	−5.87	0.17	1.31	−27.88	−28.61	−29.18	0.300	−8.89
3KXN	−34.97	−4.90	1.02	−6.53	−32.32	−38.32	−31.88	0.023	−10.41
R^2	0.83	0.79	0.20			0.76[d]	0.96		

Test Set B

	CK2-Inhibitor Binding Energy								
Inhibitor	PM6-DH2X[b]					AMBER		K_i (μM)[b]	ΔG_{exp}
	ΔH_w	$\Delta\Delta G_w$(I)	ΔE_{def}(I)	$T\Delta S_w$	$\Delta G'_w$	MM-GBSA//MM-SS[c]	MM-GBSA//MM-MD		
4a	−21.21	−2.57	0.11	−10.28	−13.39	−29.92	−26.30	0.460	−8.64
8a	−18.93	−2.55	0.12	−6.58	−14.78	−32.00	−28.45	0.330	−8.83
10a	−17.56	−4.87	0.42	−14.24	−7.77	−38.75	−34.12	0.120	−9.43
12a	−21.99	−5.70	1.21	−9.14	−17.34	−39.97	−34.00	0.120	−9.43
13a	−22.76	−5.99	0.25	−11.52	−16.97	−40.39	−35.72	0.090	−9.60
15	−18.88	−9.21	0.89	−13.28	−13.92	−43.01	−35.78	0.050	−9.95
K10	−17.21	−4.23	0.11	−13.59	−7.75	−29.73	−26.07	0.370	−8.76
K22	−16.50	−10.64	0.46	−15.98	−10.70	−35.27	−30.23	0.200	−9.13
R^2	−0.12	0.38	−0.06			0.96	0.92		

[a]Binding energy components of MM-GBSA are given as Supporting Information. [b]PM6-DH2X energy components and K_i values were taken from ref 27. [c]Single-structure (SS) here refers to the energy−minimized crystal structure, if available, or energy−minimized docked structure. [d]1J91 was not considered during the R^2 calculation.

places and compared to the corresponding BSSE-corrected MP2 level with a mixed basis set scheme: the aug-cc-pVDZ-PP basis set for the Br and I atoms and the aug-cc-pVDZ basis set for all the other atoms (see Table 1).

The dissociation curves of the studied halobenzene complexes at the PM6-DH2X and AMBER empirical levels agree well with the corresponding MP2 curves. For chlorobenzene complexes, the AMEBR force field describes the halogen bond geometry better than the PM6-DH2X method, relative to the MP2 level; the calculated rms errors are 0.09 and 0.24 Å for the AMBER and PM6-DH2X levels, respectively, with respect to the MP2 level. The rms error in the halogen bond energy calculated at the empirical level is nearly the same as that calculated at the PM6-DH2X level, 0.37 and 0.32 kcal/mol^2, respectively, with respect to the MP2 level.

For bromobenzene complexes, however, the PM6-DH2X method outperforms the AMBER force field in describing the halogen bond length compared to the MP2 level (the rms errors are 0.09 and 0.20 Å for PM6-DH2X and AMBER, respectively), the AMBER force field yields a halogen bonding

dx.doi.org/10.1021/jp3003905 | J. Phys. Chem. B 2012, 116, 3659−3669

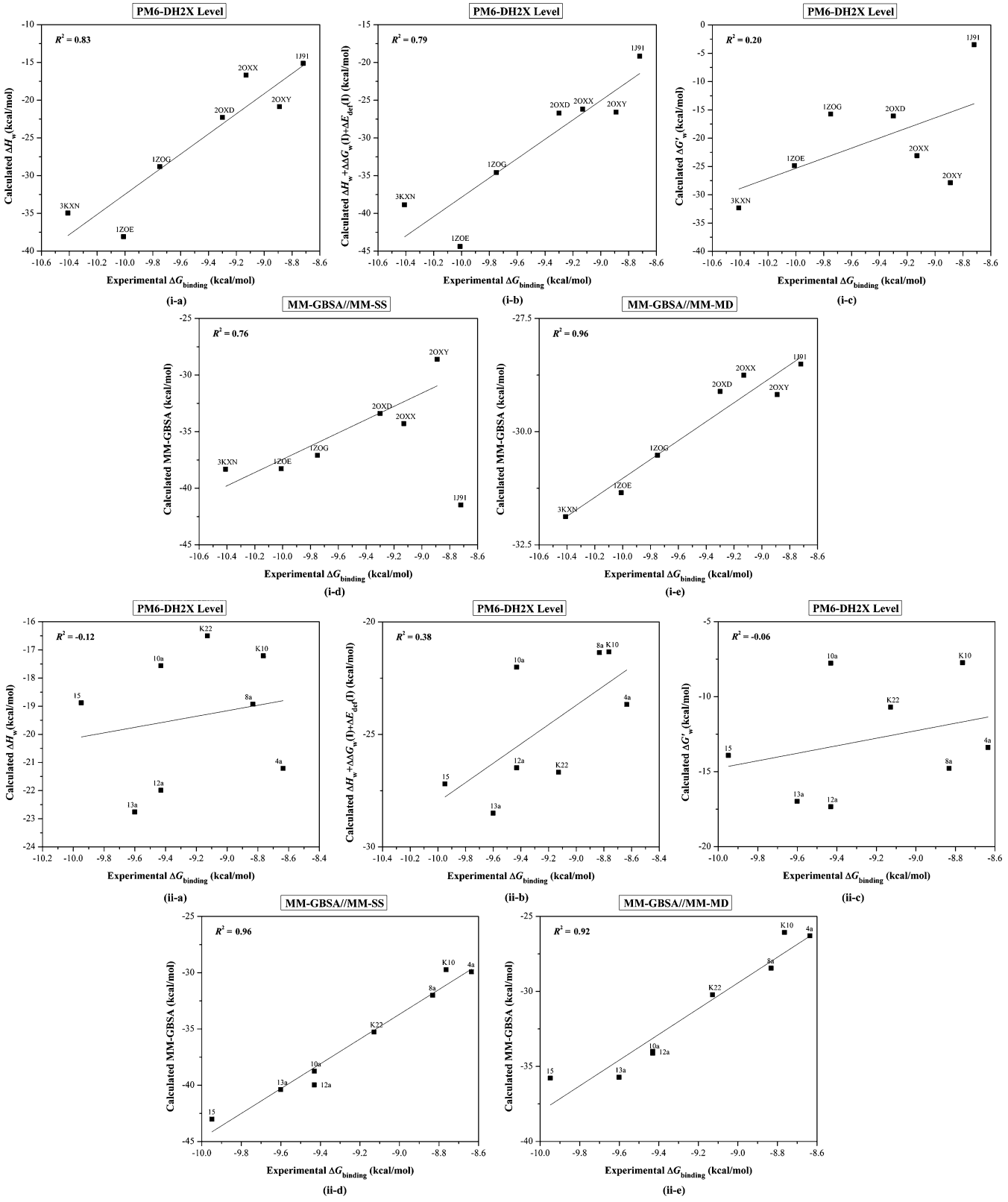

Figure 3. Calculated binding energies: (a) PM6-DH2X: interaction enthalpy, (b) PM6-DH2X: sum of the interaction enthalpy, inhibitor deformation, and corrections for the desolvation energies, (c) PM6-DH2X: total binding energy, (d) MM-GBSA//MM-SS, and (e) MM-GBSA//MM-MD for (i) test set A and (ii) test set B correlated to the experimental binding energies. In part i-d, 1J91 was not considered during the R^2 calculation.

energy closer to the corresponding MP2 level than PM6-DH2X does (the rms errors are 0.27 and 0.53 kcal/mol for AMBER and PM6-DH2X, respectively).

For iodobenzene complexes, the AMBER force field yields similar rms errors as PM6-DH2X does, relative to the MP2 level; the errors are 0.20 and 0.23 Å for the halogen bond

dx.doi.org/10.1021/jp3003905 | J. Phys. Chem. B 2012, 116, 3659–3669

Table 3. Measured halogen bond lengths and angles for the studied CK2-inihbitor complexes

Test Set A								
	halogen bond length (Å)				halogen bond angle (deg)			
			AMBER				AMBER	
inhibitor	X-ray	PM6-DH2X	MM-SS	MM-MD[a]	X-ray	PM6-DH2X	MM-SS	MM-MD[a]
1J91	4.58	–	4.52	6.51	178.6	NA	143.8	158.2
	3.99[b]	4.20[b]	4.10[b]	4.55[b]	119.6[b]	NA	149.5[b]	150.9[b]
	2.99[c]	3.12[c]	4.14[c]	3.80[c]	165.3[c]	NA	150.8[c]	83.64[c]
1ZOE	3.24	3.22	3.28	3.40	175.6	NA	173.8	168.1
1ZOG	2.98	3.06	–	–	175.3	NA	–	–
	3.27	–	3.84	3.74	173.2	–	160.8	157.1
2OXD	2.80	2.98	3.27	3.45	176.0	NA	172.3	165.8
2OXX	2.72	2.86	3.10	3.47	175.6	NA	178.4	165.0
2OXY	2.95	3.04	3.41	3.52	176.3	NA	174.0	165.1
3KXN	2.94	–	3.35	3.42	159.7	–	–	–
	3.17	3.06	–	–	172.9	NA	170.5	171.9
Test Set B								
	halogen bond length (Å)				halogen bond angle (deg)			
			AMBER				AMBER	
inhibitor	X-ray	PM6-DH2X	MM-SS	MM-MD[a]	X-ray	PM6-DH2X	MM-SS	MM-MD[a]
4a	NA	3.04	3.04	3.29	NA	NA	165.6	167.2
8a	NA	3.04	3.48	3.75	NA	NA	169.3	163.7
10a	NA	2.89	3.18	3.28	NA	NA	174.9	173.4
12a	NA	2.94	3.14	3.29	NA	NA	176.4	172.1
13a	NA	2.96	3.16	3.34	NA	NA	175.4	170.7
15	NA	2.94	3.17	3.33	NA	NA	175.3	171.6
K10	NA	3.07	3.50	3.81	NA	NA	175.2	171.9
K22	NA	3.08	3.11	3.44	NA	NA	176.9	167.4

[a]Average value. [b]Measured with respect to VAL45 residue. [c]Measured with respect to ARG47 residue.

length and 0.63 and 0.71 kcal/mol for the bond energy for the PM6-DH2X and AMBER empirical levels, respectively.

The total rms errors for the halogen bond lengths of the studied complexes were 0.19 and 0.18 Å for the PM6-DH2X and AMBER empirical levels, respectively, with respect to the MP2 level. The total rms errors for the halogen bond energy were 0.51 and 0.49 kcal/mol for the PM6-DH2X and AMBER empirical levels, respectively, with respect to the MP2 level.

Note that PM6-DH2X performs poorly compared to the AMBER and MP2 levels in the long-range regime (right side of the local minimum, see Figure 2). This is obvious in the chloro- and bromobenzene···formaldehyde dissociation curves. This observation can be attributed to the unbalanced estimation of the corrected energy components in the total PM6-DH2X energy.

In summary, the AMBER force field produces results comparable to if not better than those of the PM6-DH2X method in describing the geometry and energy of halogen bonds in halogen-bond-forming complexes. Moreover, the AMBER empirical potential incurs a much lower computational cost than the semiempirical PM6-DH2X method.

CK2-Inhibitor Complexes. PM6-DH2X and AMBER described the halogen bond properties of halogen-bond-forming complexes well compared to the MP2 level. Their performance in predicting the binding energy and halogen bond properties of CK2-inhbitor complexes was also examined.

CK2, a member of protein kinase family, enhances a tumor's phenotype by affording favorable conditions for tumorigenesis.[48] CK2-inhibitors are thought to be promising antitumor drugs. Halogenated inhibitors such as polyhalogenobenzimidazole and -benzotriazole are common class of CK2-inhibitors;[49−55] they act by forming halogen bonds primarily with the carbonyl oxygen of the amino acid residues in the hinge region of CK2.[50−52,56]

The binding affinity and molecular geometry of 15 polyhalogenated benzimidazole inhibitors complexed to CK2 protein were studied at the AMBER potential level. For the AMBER empirical calculations, two levels of structure representation were used during the MM-GBSA binding energy calculations of the CK2-inhibitors: MM-GBSA//MM-SS and MM-GBSA//MM-MD. The calculated binding energies are given in Table 2 along with the corresponding PM6-DH2X binding energies and their components. The correlations between the calculated MM-GBSA (and PM6-DH2X) and the experimental data are shown in Figure 3.

For test set A, the correlation coefficient (R^2) with respect to the experimental data for the calculated MM-GBSA binding energies was 0.76 on the basis of a single-structure molecular representation and 0.96 on the basis of MD snapshots collected over 2 ns. The MM-GBSA//MM-MD approach is believed to have outperformed the corresponding MM-MGBS//MM-SS approach because the binding energy was calculated on the basis of an ensemble of different configurations of the molecular system. On the other hand, the relatively poor performance of MM-GBSA//MM-SS is attributed to the removal of crystallic water molecules and metal ions in MM-SS calculations, which is expected to play an important role in the binding mode and energy.[56,57] The latter explanation could also account for the

dx.doi.org/10.1021/jp3003905 | J. Phys. Chem. B 2012, 116, 3659−3669

poor correlation for 1J91 which has a water molecule at the active site as calculated at MM-GBSA//MM-SS.

The MM-GBSA//MM-MD binding energies are much better correlated with the experimental data than the PM6-DH2X binding energies; R^2 is 0.83 for PM6-DH2X and 0.96 for MM-GBSA//MM-MD. Note that the R^2 value for PM6-DH2X corresponds to the correlation between the enthalpy interaction of the studied systems at the PM6-DH2X level and the experimental data. The inclusion of the solvation energy and deformation energy and entropy energy components decreases the correlation coefficients to 0.79 and 0.20, respectively.

For test set B, MM-GBSA dramatically outperformed PM6-DH2X in predicting the binding energies of the studied inhibitors; the correlation between the binding energy predicted by PM6-DH2X and the experimental data decreased from 0.83 for test set A to −0.12 for test set B. The best predictions using PM6-DH2X were obtained by accounting for the solvation and deformation energies; the correlation coefficient in this case was 0.38 with respect to the experimental data.

On the other hand, the MM-SS approach predicted the binding energy for test set B (R^2 = 0.96) better than for test set A (R^2 = 0.76). This improved performance can be attributed to the fact that the initial molecular structures of the complexes in test set B were generated on the basis of a single PDB crystal structure, decreasing the effect of the absence of a water molecule (and/or metal ions) in the active site on the binding mode (and binding energy). Moreover, the calculated binding energies based on MM-MD agree well with the experimental data (R^2 = 0.92).

The MM-GBSA binding energies for test sets A and B based on the energy minimized single-structure and uncorrelated snapshots collected from the MD simulation generally show higher correlation with the experimental data than the corresponding PM6-DH2X binding energies.

To study the halogen bond stability after minimization or during the MD simulation, the halogen bond length between the inhibitor's halogen atom and the carbonyl oxygen of the VAL114 residue in the active site was measured. Because the halogen bond is defined as a directional noncovalent bond between a halogen atom and a Lewis base, the halogen bond angle was also considered. It should be pointed out that, in the MD calculations, the rotation of the inhibitor inside the active site of the CK2 protein was considered; therefore, the halogen bond length and angle were measured between the carbonyl oxygen of the amino acid residue and the closest inhibitor's halogen atom. The measured halogen bond lengths and angles are given in Table 3. The corresponding PM6-DH2X and crystal structure data are given for comparison.

The calculated distances between the studied inhibitor's halogen atom and the carbonyl oxygen of VAL114 at the MM-SS and MM-MD levels of the molecular structure representations agree well with the experimental data and are slightly longer than those in PM6-DH2X data. On the other hand, the corresponding halogen bond angles measured at the MM-SS and MM-MD levels range from 160 to 180°, this is consistence with the X-ray data and the range of halogen bond angles in biological molecules, which is 145−180°.[58] No information about the halogen bond angle at the PM6-DH2X level is available for comparison to the AMBER results.[27]

The halogen bond length in the minimized MM-SS structure of the CK2−1J91 complex exceeded 4.0 Å. The poor description of the halogen bond here can be attributed to the absence of crystallic water molecules in the active site, as discussed above.

Limitations of the PM6-DH2X Level. Water molecules and aromatic rings in biological systems play a crucial role in identifying the binding mode and/or estimating the binding energy of inhibitors inside active sites. In addition to the traditional noncovalent halogen···Lewis base interaction, halogens interact to the benzene rings in orthogonal position, forming C−X···π-system interaction.[59,60] On the other hand, halogens form hydrogen bonds with Lewis acids (e.g., water and benzene molecules) with C−X···H bond angles of $90° \leq \theta \leq 120°$.[7,61,62]

The current study examined these types of noncovalent interactions. Specifically, we examined the ability of PM6-DH2X and AMBER empirical levels to describe the geometry and energy of noncovalent interactions in halobenzene··· benzene (C−X···π-system, Figure 4a), benzene···halobenzene

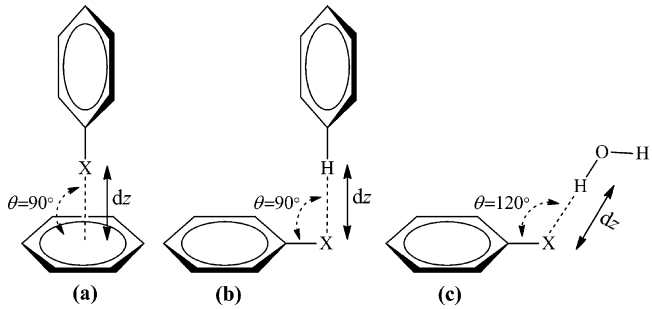

Figure 4. Schematic representation of halobenzene interactions with (a) benzene ring: C−X···π-system, (b) benzene molecule: C−X···H−C, and (c) water molecule: C−X···H−O.

(C−X···H−C, Figure 4b), and halobenzene···water (C−X···H−O, Figure 4c). The potential energy dissociation curves of these complexes were calculated at the PM6-DH2X and AMBER empirical levels; the results were compared to the corresponding data for the BSSE-corrected MP2/aug-cc-pVDZ level (with polarization functions on the Br and I atoms). The dissociation curves are plotted in Figure 5, and the calculated bond lengths and binding energies are given in Table 4.

It is worth to mention out that the halogen-bond-correction term in the PM6-DH2X method has parameters for neither C−X···C nor C−X···H. As a result, the performance of the PM6-DH2X method for these two noncovalent interactions is expected to be the same as that of PM6-DH2.

In halobenzene···benzene complexes, the PM6-DH2 method failed to predict the C−X···π-system noncovalent interaction; it overestimated the corresponding binding energy in the iodo and bromo complexes and yielded an inaccurate potential energy surface with two local minima in the chloro complex, Figure 5i.

Furthermore, the PM6-DH2 method failed to predict the correct order of hydrogen bond strengths in halobenzene···· water complexes, yielding the strength of the hydrogen bond for the iodo complexes stronger than that for the corresponding bromo complex (Cl ≈ I > Br). On the other hand, accounting for the halogen-bond correction for C−X···O_{water} did not correct the failure of PM6-DH2 to describe hydrogen bond interactions involving halogen atoms. The poor performance of the PM6-DH2 method in describing the hydrogen bond in C−X···H−C in benzene···halobenzene complexes was also marked (I > Cl > Br); see Table 4 and Figure 5.

dx.doi.org/10.1021/jp3003905 | J. Phys. Chem. B 2012, 116, 3659−3669

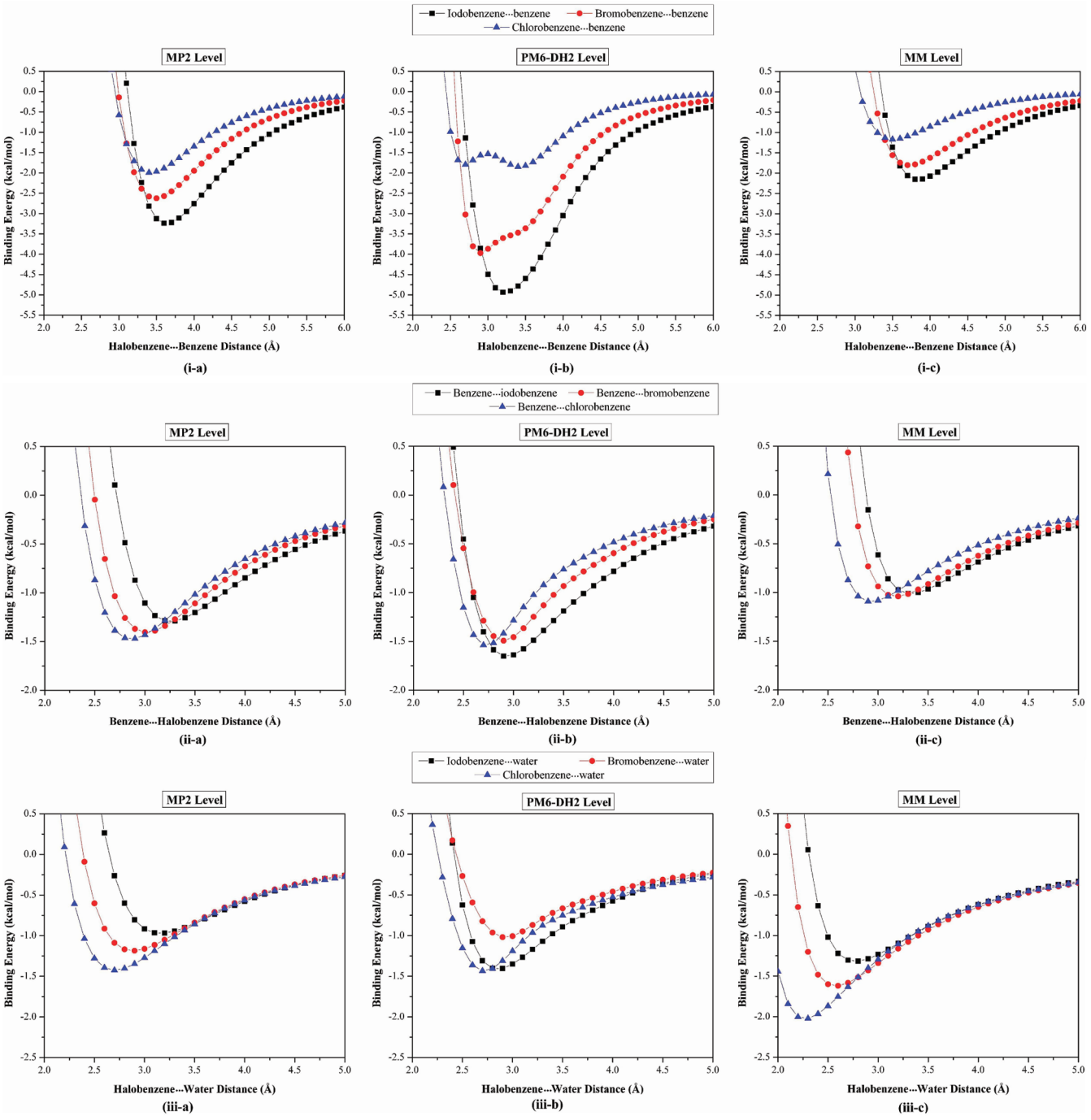

Figure 5. Potential energy dissociation curves for (i) halobenzene···benzene (C−X···π-system), (ii) benzene···halobenzene (C−X···H−C), and (iii) halobenzene···water (C−X···H−O) complexes calculated (a) at BSSE-corrected MP2/aug-cc-pVDZ level (with PP functions on the Br and I atoms), (b) by PM6-DH2X method, and (c) by AMBER force field.

In contrast, the AMBER force field performed well for C−X···H−C/O noncovalent interactions; it predicted the correct hydrogen bond order (Cl > Br > I) and the predicted bond properties agree well with those of the MP2 level.

In C−X···π-system complexes, the measured bond length was slightly longer at the AMBER empirical level than at the MP2 level: ∼0.2 Å longer in the studied halo complexes. To better understand this observation, a parallel calculation was performed on the potential energy dissociation curve for benzene···benzene forming hydrogen bond type of C−H···π-system. The potential energy curves are given as Supporting Information. The AMBER force field yielded a hydrogen bond length of 2.63 Å with bond energy of −2.01 kcal/mol, whereas the hydrogen bond length and energy calculated at the MP2 level were 2.46 Å and −3.17 kcal/mol, respectively. This explains the source of the ∼0.2 Å longer C−X···π-system bond at the AMBER empirical level and confirms the good performance of our developed PEP approach for halogen bonding. On the other hand, the short hydrogen bond lengths compared to the MP2 level in the studied halobenzene···water complexes using the AMBER force field are attributed to the fact that the HW atom type of the hydrogen atom in the TIP3P water molecule has no van der Waals radius. This was confirmed by the fact that the hydrogen bond lengths in benzene···

dx.doi.org/10.1021/jp3003905 | J. Phys. Chem. B 2012, 116, 3659−3669

Table 4. Calculated Bond Lengths of, and Energies for, Halobenzene Molecules Complexed to Water and Benzene Molecules

	bond length (Å)[a]			bond energy (kcal/mol)		
system	MP2	PM6-DH2	AMBER	MP2	PM6-DH2	AMBER
chlorobenzene···benzene (C−X···π-system)[a]	3.42	3.42 (2.68)[b]	3.51	−1.99	−1.85 (−1.80)[b]	−1.17
bromobenzene···benzene (C−X···π-system)[a]	3.49	2.89	3.72	−2.63	−3.97	−1.81
iodobenzene···benzene (C−X···π-system)[a]	3.63	3.22	3.84	−3.24	−4.94	−2.16
benzene···chlorobenzene (C−X···H−C)	2.86	2.73	2.93	−1.47	−1.54	−1.09
benzene···bromobenzene (C−X···H−C)	3.01	2.90	3.18	−1.41	−1.49	−1.04
benzene···iodobenzene (C−X···H−C)	3.26	2.93	3.32	−1.29	−1.65	−1.01
chlorobenzene···water (C−X···H−O)	2.70	2.71 (2.72)[c]	2.27	−1.43	−1.44 (−1.43)[c]	−2.03
bromobenzene···water (C−X···H−O)	2.89	2.93 (2.98)[c]	2.58	−1.19	−1.02 (−0.91)[c]	−1.62
iodobenzene···water (C−X···H−O)	3.16	2.85 (2.89)[c]	2.77	−0.97	−1.41 (−1.34)[c]	−1.32

[a]Bond length measured as the distance between the halogen atom and the centroid of the benzene ring. [b]Two local minima were observed; see Figure 5. [c]Bond length/energy calculated at the PM6-DH2 level with accounting for C−X···O_{water} correction.

halobenzene complexes agree well with the MP2 data (rms error of ∼0.1 Å).

CONCLUSION

The current study was designed to re-evaluate the performance of the AMBER empirical potential and PM6-DH2X method in describing the halogen bond properties of halobenzene···Lewis base and CK2-inhibitor complexes. In the AMBER calculations, we employed our developed PEP approach of representing the σ-hole with an extra-point of charge. The results showed that both the AMBER force field and the PM6-DH2X method predict the halogen bond properties well in the studied halobenzene···Lewis base complexes compared to the BSSE-corrected MP2/aug-cc-pVDZ level (with PP functions on the Br and I atoms). AMBER predicted the binding energy of 15 polyhalogenated benzimidazole inhibitors complexed to CK2 proteins much better than the PM6-DH2X method did. Finally, the ability of both methods to describe other important noncovalent halogen interactions, such as C−X···π-system and C−X···H−O/C interactions, was assessed. The PM6-DH2X method failed to describe those types of interactions, yielding the incorrect order of hydrogen bond strength in the studied C−X···H−O/C complexes and an inaccurate potential energy surface for the C−X···π-system complexes. However, the AMBER force field performed well. A further correction to PM6-DH2X for noncovalent halogen interactions should be developed and evaluated.

ASSOCIATED CONTENT

Supporting Information

Information concerning the energy components of the MM-GBSA binding energies and the potential energy curves for benzene dissociation (C−H···π-system). This material is available free of charge via the Internet at http://pubs.acs.org.

AUTHOR INFORMATION

Corresponding Author

*E-mail: m.ibrahim@compchem.net.

Notes

The authors declare no competing financial interest.

ACKNOWLEDGMENTS

The author would like to acknowledge the School of Chemistry, The University of Manchester, for supporting the author's research in various ways. The author would like to thank J. Řezáč and J. Stewart for their assistance with setting up the PM6-DH2X calculations. This work was supported by the Egyptian Ministry of Higher Education & Scientific Research.

DEDICATION

†This article is dedicated to the AMBER teamwork and mailing list.

REFERENCES

(1) Gavezzotti, A. *Mol. Phys.* **2008**, *106*, 1473−1485.
(2) Lu, Y.; Wang, Y.; Zhu, W. *Phys. Chem. Chem. Phys.* **2010**, *12*, 4543−4551.
(3) Lu, Y.; Shi, T.; Wang, Y.; Yang, H.; Yan, X.; Luo, X.; Jiang, H.; Zhu, W. *J. Med. Chem.* **2009**, *52*, 2854−2862.
(4) Metrangolo, P. *Angew. Chem., Int. Ed.* **2008**, *47*, 6114−6127.
(5) Politzer, P.; Lane, P.; Concha, M.; Ma, Y.; Murray, J. *J. Mol. Model.* **2007**, *13*, 305−311.
(6) Clark, T.; Hennemann, M.; Murray, J.; Politzer, P. *J. Mol. Model.* **2007**, *13*, 291−296.
(7) Politzer, P.; Murray, J. S.; Clark, T. *Phys. Chem. Chem. Phys.* **2010**, *12*, 7748−7757.
(8) Alkorta, I.; Blanco, F.; Solimannejad, M.; Elguero, J. *J. Phys. Chem. A* **2008**, *112*, 10856−10863.
(9) Aakeröy, C. B.; Fasulo, M.; Schultheiss, N.; Desper, J.; Moore, C. *J. Am. Chem. Soc.* **2007**, *129*, 13772−13773.
(10) Metrangolo, P.; Neukirch, H.; Pilati, T.; Resnati, G. *Acc. Chem. Res.* **2005**, *38*, 386−395.
(11) Palusiak, M. *J. Mol. Struct. THEOCHEM* **2010**, *945*, 89−92.
(12) Wang, W.; Wong, N.-B.; Zheng, W.; Tian, A. *J. Phys. Chem. A* **2004**, *108*, 1799−1805.
(13) Lu, Y.-X.; Zou, J.-W.; Wang, Y.-H.; Yu, Q.-S. *J. Mol. Struct. THEOCHEM* **2006**, *776*, 83−87.
(14) Politzer, P.; Murray, J.; Concha, M. *J. Mol. Model.* **2008**, *14*, 659−665.
(15) Jabłoński, M.; Palusiak, M. *J. Phys. Chem. A* **2012**, DOI: 10.1021/jp211606t.
(16) Grabowski, S. J. *J. Phys. Chem. A* **2012**, DOI: 10.1021/jp2109303.
(17) Lu, Y.-X.; Zou, J.-W.; Wang, Y.-H.; Jiang, Y.-J.; Yu, Q.-S. *J. Phys. Chem. A* **2007**, *111*, 10781−10788.
(18) Li, R.-Y.; Li, Z.-R.; Wu, D.; Li, Y.; Chen, W.; Sun, C.-C. *J. Phys. Chem. A* **2005**, *109*, 2608−2613.
(19) An, X.; Jing, B.; Li, Q. *J. Phys. Chem. A* **2010**, *114*, 6438−6443.
(20) Yun-Xiang, L.; Jian-Wei, Z.; Ji-Cai, F.; Wen-Na, Z.; Yong-Jun, J.; Qing-Sen, Y. *J. Comput. Chem.* **2009**, *30*, 725−732.
(21) Murray, J.; Lane, P.; Clark, T.; Riley, K.; Politzer, P. *J. Mol. Model.* **2011**, *18*, 541−548.
(22) Dong, X.-f.; Ren, F.-d.; Cao, D.-l.; Wang, W.-n.; Zhang, F.-q. *J. Mol. Struct. THEOCHEM* **2010**, *961*, 73−82.
(23) Ibrahim, M. A. A. *J. Chem. Inf. Model.* **2011**, *51*, 2549−2559.
(24) Stewart, J. *J. Mol. Model.* **2007**, *13*, 1173−1213.

(25) Stewart, J. *J. Mol. Model.* **2009**, *15*, 765−805.
(26) Řezáč, J.; Hobza, P. *Chem. Phys. Lett.* **2011**, *506*, 286−289.
(27) Dobeš, P.; Řezáč, J.; Fanfrlík, J.; Otyepka, M.; Hobza, P. *J. Phys. Chem. B* **2011**, *115*, 8581−8589.
(28) Ibrahim, M. A. A. *J. Comput. Chem.* **2011**, *32*, 2564−2574.
(29) Møller, C.; Plesset, M. S. *Phys. Rev.* **1934**, *46*, 618−622.
(30) Dunning, J. T. H. *J. Chem. Phys.* **1989**, *90*, 1007−1023.
(31) Woon, D. E.; Dunning, J. T. H. *J. Chem. Phys.* **1993**, *98*, 1358−1371.
(32) Riley, K. E.; Merz, K. M. *J. Phys. Chem. A* **2007**, *111*, 1688−1694.
(33) Boys, S. F.; Bernardi, F. *Mol. Phys.* **1970**, *19*, 553−566.
(34) Frisch, M. J.; Trucks, G. W.; Schlegel, H. B.; Scuseria, G. E.; Robb, M. A.; Cheeseman, J. R.; Montgomery, J. A.; Vreven, T.; Kudin, K. N.; Burant, J. C.; et al. *Gaussian 03*; Gaussian, Inc.: Wallingford CT, 2004.
(35) Bayly, C. I.; Cieplak, P.; Cornell, W.; Kollman, P. A. *J. Phys. Chem.* **1993**, *97*, 10269−10280.
(36) Jorgensen, W. L.; Severance, D. L. *J. Am. Chem. Soc.* **1990**, *112*, 4768−4774.
(37) Jorgensen, W. L.; Chandrasekhar, J.; Madura, J. D.; Impey, R. W.; Klein, M. L. *J. Chem. Phys.* **1983**, *79*, 926−935.
(38) Stewart, J. J. P.; Stewart Computational Chemistry: Colorado Springs, CO, 2008.
(39) Becke, A. D. *Phys. Rev. A* **1988**, *38*, 3098−3100.
(40) Lee, C.; Yang, W.; Parr, R. G. *Phys. Rev. B* **1988**, *37*, 785−789.
(41) Krishnan, R.; Binkley, J. S.; Seeger, R.; Pople, J. A. *J. Chem. Phys.* **1980**, *72*, 650−654.
(42) Niefind, K.; Guerra, B.; Ermakowa, I.; Issinger, O.-G. *EMBO J.* **2001**, *20*, 5320−5331.
(43) Morales, J. L.; Nocedal, J. *SIAM J. Optim.* **2000**, *10*, 1079−1096.
(44) Case, D. A.; Darden, T. A.; Cheatham, T. E., I. I. I.; Simmerling, C. L.; Wang, J.; Duke, R. E.; Luo, R.; Crowley, M.; Walker, R. C.; Zhang, W.; et al. *AMBER 10*; University of California: San Francisco, 2008.
(45) Hornak, V.; Abel, R.; Okur, A.; Strockbine, B.; Roitberg, A.; Simmerling, C. *Proteins: Struct. Funct. Bioinf.* **2006**, *65*, 712−725.
(46) Wang, J.; Wolf, R. M.; Caldwell, J. W.; Kollman, P. A.; Case, D. A. *J. Comput. Chem.* **2004**, *25*, 1157−1174.
(47) Sitkoff, D.; Sharp, K. A.; Honig, B. *J. Phys. Chem.* **1994**, *98*, 1978−1988.
(48) Sarno, S.; Pinna, L. A. *Mol. BioSyst.* **2008**, *4*, 889−894.
(49) Pagano, M. A.; Andrzejewska, M.; Ruzzene, M.; Sarno, S.; Cesaro, L.; Bain, J.; Elliott, M.; Meggio, F.; Kazimierczuk, Z.; Pinna, L. A. *J. Med. Chem.* **2004**, *47*, 6239−6247.
(50) Battistutta, R.; Mazzorana, M.; Sarno, S.; Kazimierczuk, Z.; Zanotti, G.; Pinna, L. A. *Chem. Biol.* **2005**, *12*, 1211−1219.
(51) Gianoncelli, A.; Cozza, G.; Orzeszko, A.; Meggio, F.; Kazimierczuk, Z.; Pinna, L. A. *Bioorg. Med. Chem.* **2009**, *17*, 7281−7289.
(52) Zien, P.; Duncan, J. S.; Skierski, J.; Bretner, M.; Litchfield, D. W.; Shugar, D. *BBA—Proteins Proteomics* **2005**, *1754*, 271−280.
(53) Szyszka, R.; Grankowski, N.; Felczak, K.; Shugar, D. *Biochem. Biophys. Res. Commun.* **1995**, *208*, 418−424.
(54) Dobrowolska, G.; Muszynska, G.; Shugar, D. *BBA—Protein Struct. M.* **1991**, *1080*, 221−226.
(55) Andrzejewska, M.; Pagano, M. A.; Meggio, F.; Brunati, A. M.; Kazimierczuk, Z. *Bioorg. Med. Chem.* **2003**, *11*, 3997−4002.
(56) Mazzorana, M.; Pinna, L.; Battistutta, R. *Mol. Cell. Biochem.* **2008**, *316*, 57−62.
(57) Battistutta, R.; Mazzorana, M.; Cendron, L.; Bortolato, A.; Sarno, S.; Kazimierczuk, Z.; Zanotti, G.; Moro, S.; Pinna, L. A. *ChemBioChem* **2007**, *8*, 1804−1809.
(58) Auffinger, P.; Hays, F. A.; Westhof, E.; Ho, P. S. *Proc. Natl. Acad. Sci. U.S.A.* **2004**, *101*, 16789−16794.
(59) Shishkin, O. V. *Chem. Phys. Lett.* **2008**, *458*, 96−100.
(60) Duarte, D.; de las Vallejos, M.; Peruchena, N. *J. Mol. Model.* **2010**, *16*, 737−748.
(61) Brammer, L.; Bruton, E. A.; Sherwood, P. *Cryst. Growth Des.* **2001**, *1*, 277−290.
(62) Brinck, T.; Murray, J. S.; Politzer, P. *Int. J. Quantum Chem.* **1992**, *44*, 57−64.